PB2004-105288

Analysis of Industrial Noise for Hearing Conservation

Sheau-Fang Lei, Ph.D.

Project Director

Submitted in partial fulfillment of:

Grant Number 1-K01-OH00139

for the

Project Period 30 September 1994 through 29 September 1997

Auditory Research Laboratories
Plattsburgh State University
101 Broad Street
Plattsburgh, NY 12901

TABLE OF CONTENTS

I. Specific Aims

Noise measurements made for the purpose of hearing conservation practice, have as their objective the extraction of some physical metric from the noise that can be used to estimate the hazards to hearing from prolonged exposure to that noise. Unlike other areas of environmental monitoring, the substantive aspects (as opposed to the purely technological) of noise measurement practice have not evolved with the improvements in signal analysis capabilities. Current practice continues to rely primarily upon a time averaged, integrated approach to quantifying a noise exposure, i.e., essentially a measure of the frequency weighted average energy of an exposure. Temporal variables are completely neglected. In fact, a variety of recent experiments have shown that an understanding of the temporal structure of a noise is critical to predicting the hazard to hearing. An argument, based upon experimental evidence, was presented in our original proposal to defend the proposition that such time averaged metrics are not adequate for estimating the hazard to hearing from industrial/military noise environments. These environments are usually very complex (i.e., in the most general case, non-stationary stochastic signals) and are not adequately described by time averaged metrics.

This research grant was originally conceived as a result of the inadequacy of current measurements to deal with complex noise measurements. Its primary objective was the broadly stated goal of using relatively new signal analysis techniques to extract metrics from a continuously sampled acoustic signal that can be used in conjunction with or as an alternative to the traditional metrics to provide a more adequate assessment of the hazard of a noise measurement. The following metrics, that can be used to quantify industrial noises, were developed as a result of this grant: (1) Frequency domain kurtosis (FDK), on any preselected frequency scale, provides an indication of which regions of the energy spectrum undergo fluctuations and the extent of these fluctuations relative to Gaussian conditions. (2) The joint peak-interval histogram which will identify each impulsive level, within a predetermined peak bin, with its interpeak interval distribution. From this surface conventional peak and interval histograms have been obtained. The above metrics were obtained by applying two algorithms based on signal processing techniques; the wavelet transform and higher-order cumulant based inverse filtering. These algorithms also yield the distribution of time domain kurtosis.

II. Significant Findings

The accumulating experimental data on noise-induced hearing loss (NIHL) has shown that conventional energy-based metrics used to quantify industrial noise may be necessary but not sufficient for the evaluation of hearing hazards. The objectives of this grant were to explore new and more generalized ways of quantifying industrial noise environments, especially those approaches that would result in metrics which incorporate the temporal and statistical properties of a nonGaussian noise. The metrics [frequency and time domain kurtosis and the joint peak-interval histogram] and the methods by which they can be obtained were developed as a result of this grant.

These metrics can differentiate among noises that have the same energy and spectra but in general very different temporal patterns which have a profound effect on hearing hazard.

Frequency domain kurtosis was obtained from an application of wavelet analysis to the noise waveform. While higher-order cumulant based inverse filtering was used to extract timing and peak amplitude information from a noise waveform having randomly occurring transient components. From this analytical process the joint peak-interval histogram was obtained from which the cumulative distribution of both the timing and peak amplitudes of the repetitive components in a time-varying and highly nonGaussian waveform were also obtained; i.e., a timing interval histogram for a given amplitude or a peak amplitude histogram for a given interval was derived from the joint peak-interval histogram.

Both of these analytical procedures can be incorporated into digital noise measurement systems.

III. Usefulness of Findings

Considerable research data gathered over the last several decades has shown the complexity of NIHL. A number of animal model experiments clearly show the significant role of temporal variables of a noise stimulus in the degradation of hearing. However, the development of new metrics based on these experimental findings has not been forthcoming. The temporal/statistically based metrics produced as a result of this grant (FDK and joint peak-interval histogram metrics), in conjunction with the energy metrics can provide a more complete set of measurement tools for evaluating noise environments in the assessment of the hazards to hearing. What remains to be done is to exhaustively test these metrics in an animal model of NIHL in order to evaluate their predictive value. If substantially improved correlations among cochlear pathology, measures of hearing and the new noise metrics are found, these new metrics can be incorporated into computer-based instrumentation for evaluating industrial noise environments. These metrics may also have engineering applications for identifying features of the noise that can be reduced at their source or for incorporation into the design of hearing protective devices.

IV. Background

(a) The Wavelet transform: The wavelet transform (WT) was originally introduced to signal analysis by the French geophysicist J. Morlet (1982). Since then it has received considerable attention where it has become an essential tool for researchers and engineers involved in signal processing. The WT is defined by integration of a signal and a set of basis functions as shown in (1).

$$W(a,b) = \frac{1}{\sqrt{a}} \int x(t)\, \overline{\Psi}\left(\frac{t-b}{a}\right) dt \tag{1}$$

The bar indicates the complex conjugate. This integration operation decomposes a time varying signal x(t) in terms of a set of basis functions (or wavelets). These wavelets are obtained from a single function (the mother wavelet) by dilations (a: dilation scale) as well as translations (b: time translation). This wavelet must satisfy the admissibility condition given by:

$$\begin{aligned} &\int_{-\infty}^{\infty} \left|\Psi(t)\right|^2 dt < \infty \\ &\hat{\Psi}(\omega)\Big|_{\omega=0} = 0 \end{aligned} \tag{2}$$

where $\hat{\Psi}(\omega)$ is the Fourier transform of $\Psi(t)$. This admissibility condition implies that the mother wavelet has to have a finite energy, and be an oscillatory function. To be useful in practical applications, the mother wavelet is usually nonzero on a finite interval, or decreases rapidly as time approaches infinity. Thus the WT can decompose a signal into a time-frequency representation because the wavelets are localized in time and frequency. The WT is closely analogous to the short-time Fourier transform (STFT). The linearity of the signal decomposition makes these transforms more suitable for the analysis of multicomponent signals than are quadratic time-frequency distributions (Hlawatsch, 1992) which suffer from cross-term interferences. Unlike the STFT, the WT, which has a variable time and frequency resolution, can overcome the resolution limitation encountered by the STFT in the joint time-frequency decomposition of a nonstationary signal. This advantage is what enables the WT to decompose a signal spectrum on a logarithmic scale.

Due to the high computational burden of a direct execution of a WT in (1), the discrete WT (DWT) is desirable. The DWT was not fully developed and used until Daubechies (1989) and Mallat (1989) helped complete the framework for the theory and demonstrated the applicability of the mathematical theory to engineering problems. The DWT can be implemented efficiently using Mallat's pyramid algorithm (Mallat, 1989). The Mallat algorithm was developed for orthogonal wavelets which are associated with the form of the quadrature mirror filter banks. Therefore, the most commonly used filter pairs for Mallat's algorithm have been Daubechies filters or other restrained filters which lead to an orthogonal decomposition. An alternative approach to implementing the DWT is with the A-trous algorithm, originally proposed by Holschneider et al. (1989) for music synthesis. The A-trous algorithm allows any wavelet to be chosen for analysis without the restriction of using the orthogonal wavelets. Therefore the A-trous algorithm gives rise to non-orthogonal decompositions which have greater flexibility in applications using generalized wavelets. The A-trous algorithm (Shensa, 1992) can be implemented with pyramidal calculations having a structure similar to Mallat's algorithm. In this approach, there are two filters which function as bandpass and lowpass filters which are arranged in an iterative sequence, to form a hierarchical filter bank in the pyramidal structure that eventually yields the DWT. The coefficients for the bandpass filter are the discrete samples of the continuous wavelet function chosen for the analyzing mother wavelet provided that the coefficients of the lowpass filter f(n) satisfy the A-trous condition (3)

$$f(2n)=\delta\left(n\right)/\sqrt{2} \tag{3}$$

An acoustic signal entering the ear causes a mechanical vibration to be transmitted through the conductive structures of the external and middle ear to the fluids of the cochlea, the inner ear. The basiliar membrane within the cochlea will respond to the stimulus by producing a spatio-temporal pattern of displacements along its entire length. These displacements show a frequency sensitivity form the base to the apex; the point of the maximum displacement for high frequencies occurs near the basal end, and for low frequencies, at the wider apical end. Thus the basiliar membrane mechanics separates the incoming stimulus spectrally onto different spatial locations in a tonotopically ordered manner. Thus from the functional view, the cochlea analyzes sound much like performing a spectral decomposition through a parallel bank of auditory filters. The impulse responses of the filters maintain approximately a constant Q-factor scale, related to each other by a dilation. This naturally suggests that this stage of acoustical processing in the cochlea can be modeled as a wavelet transform (Yang et al., 1992) of the stimulus, and thus by analogy, if one would like to extract a metric from an environmental noise that will correlate with the cochlear response to that noise, the WT would seem to be an appropriate approach.

The frequency response of each filter in the auditory filterbank can be descibed as time-invariant, and linear (Cooke, 1993; Patterson, 1992) . The gammatone function is a simple and reasonably accurate linear model that has been used to simulate the impulse response of an auditory filter. The gammatone filter, as indicated by Patterson et al. (1992), offers a means of producing an auditory filterbank that fits both physiological and psychophysical data on human frequency selectivity. Holdsworth (1988) designed an efficient digital filter by taking advantage of the simple analytic form of the gammatone function. The impulse response of a gammatone filter g(t) is

$$g(t)=t^{n-1}\, e^{-2\pi bt}\, \cos\left(\omega_c + \varphi\right) u\left(t\right) \tag{4}$$

where n is the filter order, b is the damping factor related to the bandwidth (Glasberg, 1990), ω_c is the radian center frequency and u(t) is the unity step function. The impulse response and frequency spectrum of a fourth order (n=4 in (4)) gammatone filter are shown in Figures 1(a) and 1(b). The spectral magnitude of a gammatone filter has an asymmetrically-shaped response in the frequency domain. In particular, the rate of decay (roll-off) of the filter with respect to distance from the center frequency is much higher on the high frequency side than on the low frequency side. A gammatone function, as a candidate for simulating an auditory filter, can be chosen as the analyzing mother wavelet to implement the WT in order to extract the FDK metric. The A-trous algorithm for computing the WT is needed since the gammatone function is not an orthogonal wavelet kernel.

(b) Frequency domain kurtosis: Kurtosis, a fourth-order statistic, originally found useful in the measurement of helicopter and jackhammer noises (ISO 3891, 1978; Erdreich, 1986), is considered a good metric for classifying the impulsive character of continuous nonGaussian noises. The kurtosis metric, taken from the amplitude distribution of a signal, is dependent on the probability density function (PDF) of the amplitude distribution. The PDF of the amplitude distribution of an impulse has a very different shape from that of a steady-state Gaussian-distributed waveform. Most of the samples of an impulsive signal are concentrated at low amplitude levels while a few samples are at high amplitudes. For a Gaussian-distributed waveform, kurtosis will have a value around 3, while the kurtosis for a highly impulsive type of continuous noise signal can have a much greater value. Kurtosis is sensitive to the peak and background energy levels of a signal which are affected by unsteady multiple peaks, and the nonuniform interval periodicity within a signal. Kurtosis can serve as a metric which can quantify the extent of the amplitude fluctuations of a nonGaussian and nonstationary signal. For a nonstationary signal, a joint time-frequency analysis can show how the spectral content of a signal varies in time. Kurtosis estimates can be computed on the contributed amplitude distributions across different frequencies. This metric which is called frequency domain kurtosis (FDK) is an extension of the kurtosis statistic form the time to the frequency domain.

$$K_y(4,2) = \frac{E\left\{\left(X(a_f,t) - E\{X(a_f,t)\}\right)^4\right\}}{\left(E\left\{\left(X(a_f,t) - E\{X(a_f,t)\}\right)^2\right\}\right)^2} - 3 \tag{5}$$

$X(a_f, t)$ represents the signal as a function of frequency scale (a_f) and time (t); E{ . } is the mean or expected value operator . Dwyer (1982) originally used the FDK estimate to obtain additional information about the frequency components of a randomly occurring signal that the traditional power spectral estimate could not obtain. FDK is capable of detecting nonstationary and nonGaussian transients (such as impulses and unsteady harmonic components) in the presence of a background continuous Gaussian noise. Dwyer's algorithm, however, is based on Fourier analysis (DFT analysis), hence FDK results based on his algorithm yield values on a linear frequency scale. The kurtosis statistic, when applied to the results of the wavelet transform of the input signal will yield the FDK on a logarithmically scaled frequency which is more appropriate for comparison with physiological measurements of hearing.

(c) Higher-order cumulant based filtering: Complex noises, which simulate the nonstationary and nonGaussian characteristics of realistic industrial/military noise environments, have been used as experimental stimuli in our earlier animal studies of NIHL (Lei et al., 1994) and were used in the development of the metrics discussed above. The complex noise consists of a high-level primary impulsive sequence and multiple reflected components superimposed on a continuous Gaussian background noise. Such a stimulus, x(k), can be expressed as:

$$x(k) = s(k-k_0)+\alpha_1 s(k-k_1)+\alpha_2 s(k-k_2)+\cdots+n(k)$$
$$= u(k) \otimes s(k) + n(k)$$

$$u(k) = \delta(k-k0)+\alpha_1\ \delta(k-k1)+\alpha_2\delta(k-k_2)+\cdots \tag{6}$$

where ⊗ represents the convolution operator; $\delta(k)$ is the unit kronecker delta sequence; s(k) is a primary impulsive sequence; n(k) is additive Gaussian distributed noise, and u(k) is a reflectivity sequence containing information on the amplitude reflections and time delays (α_i are the reflected amplitude factors, and k_i are time delays). These factors and delays are independent random variables which control the amplitude fluctuations resulting from multipath interference, nonstationary sources, or characteristics of the propagating medium. If α_i and k_i can simultaneously be estimated from the complex noise samples alone, then α_i and k_i can be used to construct the joint peak-interval histogram. In this grant, the deconvolution operation was applied to extract the reflectivity sequence of the complex noise waveforms.

The deconvolution operation is shown in the block diagram of Figure 2. We observe the output x(k) of an unknown, possibly nonminimum phase time-invariant linear system f(k) driven by input excitation , w(k). w(k) is desired and needs to be recovered, or equivalently to identify the inverse filter g(k) of f(k). If no knowledge of f(k) is available, this kind of deconvolution operation is considered a "blind" deconvolution in signal processing. This requires the identification of both the magnitude and the phase of the system's transfer function. The magnitude can be identified using second-order moments of the output signal, x(k). However, phase identification is more complicated since it must involve the calculation of higher order moments.

A theorem (Shalvi, 1990; Cadzow, 1995, 1996) suggests a potentially important mechanism for solving the blind deconvolution problem using higher-order cumulant-based inverse filtering. This theorem indicates that the output of any time-invariant linear operator with a white noise input results in a stationary random time series and that the magnitudes of the normalized cumulants of the output are less than or equal to the magnitude of the input excitation's normalized cumulant as shown in (7).

$$|K_y(p,q)| \ \leq\ |K_w(p,q)|,\ \ K_y(p,q) = C_y(p)/|C_y(q)|^{p/q}\ ;\ \ for\ p>q \tag{7}$$

where $K_y(p,q)$ is the normalized cumulant of order (p,q) associated with output y(k), and $C_y(q)$ is the q-order cumulant of y. The required deconvolving operator must generate a response whose normalized cumulants have magnitudes that are the largest over the class of all linear operators for all integer values p and q; usually p is an even number and q is set equal to 2. Since f(k) is implicitly contained within the measured data, x(k), the maximization of the normalized cumulant must be made with respect to the the deconvolution operator's impulse response, g(k). In other words, the response normalized cumulant is dependent on the coefficients of this inverse filter, g(k). Due to the highly nonlinear nature of this dependency, it is necessary to employ nonlinear programming techniques (Shanno, 1970) to numerically compute the required maximum. Basically, a gradient based algorithm is iteratively used until convergence occurs to the maximum value judged by two criteria: (1) the gradient vector being sufficiently close to zero, or (2) the relative change in the normalized cumulant magnitude from one iteration to the next being sufficiently small. The output of the deconvolution filter yields information on the amplitude and temporal spacing (timing) of impulsive transients and allows us to construct a joint peak-interval histogram.

V. Methodology and Procedures

The complex noise described in Lei et al. (1994) and used in trhis current research was generated by computer simulation. The simulation rountines can produce purely Gaussian or nonGaussian to highly impulsive nonstationary waveforms which replicate realistic industrial noise environments. These waveforms have the feature that their statistical properties can be chosen *a priori* while maintaining equal frequency spectra and energy level. The theoretical background for synthesizing these waveforms is presented in Hsueh and Hamernik (1990, 1991). The waveforms generated by this system can be varied by their occurrences, time delays and reflected amplitudes respectively for every synthesized window. The variation of each event is controlled by different random variables which have independent probability distributions.

The A-trous algorithm was used to implement the WT analysis of the complex noise samples. This implementation allows the WT to have the filter bank structures with computational efficiency. The basic unit of the filter pairs is iteratively cascaded as shown in Figure 3. The analyzed complex noise samples are filtered by a lowpass filter which satisfies the A-trous condition in (3), and are parallel filtered by a bandpass filter to obtain the output sequences for every frequency band (octave bands were used in our work). The coefficients of this bandpass filter are the discrete samples taken from the fourth order gammatone filter. Once the output sequences of every band are grouped as a function of time we can compute the FDK value for each corresponding octave band as shown in Figure 4.

A higher-order cumulant based inverse filter is proposed for estimating the reflectivity sequence as shown in Figure 5. An inverse filter, b(k), acts as a deconvolution filter having as an input only the measured samples of x(k). The coefficients of b(k) were obtained by maximizing the magnitude of the higher-order cumulant value (the fourth-order cumulant, kurtosis, was used in this grant; higher-order cumulant values can also be applied with the same procedures). Since the higher-order cumulant values are highly nonlinear functions of the coefficients of b(k), the coefficients of the inverse filter can be obtained by an iterative numerical optimization technique using a quasi-Newton method. The converged output sequence of the deconvolution will then be an optimum estimate of the reflectivity sequence from which information on the temporal structure of the signal can be extracted.

The procedural steps for implementing the joint peak-interval histogram are shown in Figure 6. The complex noise samples are processed in consecutive segments (windows); the temporal kurtosis of every window is computed and compared with the threshold value for purely Gaussian noise to determine if the sampled window is nonGaussian. The deconvolution using higher-order cumulant based inverse filtering is analyzed to estimate the time delays and reflected amplitudes of the impulsive components for the windows in which the nonGaussian component is present (if the window is Gaussian distributed, the samples will be neglected by cumulant based inverse filtering analysis). The information on the estimated time delays and reflected amplitudes for consecutive windows was then accumulated to construct a joint peak-interval histogram.

VI. Results

(a) FDK metric: Five different complex noise waveforms were chosen to demonstrate the extraction of the FDK metric based on the WT. The five synthesized samples were defined as follows:

Signal I: Combination of Gaussian noise and shaped impulses. The spectrum of the shaped impulses was uniform from .2 to 5 kHz. The probability of impacts occurring in a 32ms window was set at 0.1.

Signal II: Similar to Signal I, except, rather than shaped impulses, Gaussian distributed noise bursts, derived from the same uniform bandwidth as used for the impacts of Signal I, were used. The probability of a burst occurring in a 32ms window was set at 0.1.

Signal III: A combination of Gaussian noise and shaped impulses. The spectrum of the shaped impulses was uniform from 1 to 4 kHz. The probability of impacts occurring in a 32 ms window was set at 0.1.

Signal IV: Similar to Signal III, except, rather than shaped impulses, a Gaussian distributed noise burst, derived from the same uniform bandwidth as used for the impacts in Signal III, were used. The probability of a burst occurring in a 32ms window was set at 0.1.

Signal V: Similar to Signal I, except that the spectra of the impulses and Gaussian noise were interchanged. The spectrum of the shaped impulses was uniform from 5 to 16 kHz, and the Gaussian noise samples were derived from the .2 to 5 kHz uniformly distributed spectrum.

Each time-history waveform from Signals I through V had equal amplitude peaks for the shaped impulses and Gaussian noise bursts. The attenuated reflected amplitude factors were not been considered in this analysis in order to simplify the simulation conditions. However, the nonGaussian and nonstationary characteristics of the waveforms of these signals were still preserved. All five of the above signals had the same energy and time-averaged spectrum uniformly distributed from .2 to 16 kHz but very different temporal patterns as shown in Figure 7. The samples of Signals I through V shown in Figure 7(a) were synthesized by computer using a sampling frequency of 32 kHz with 1024 samples per window. Each sample waveform shown in Figure 7(a) is the result of concatenating 20 windows. The synthetic signals were analyzed by the WT using the gammatone filter as the wavelet kernel. The coefficients of the bandpass filter used in computing the WT were the discrete sampled points taken from the continuous fourth-order gammatone impulse response which has an 8 kHz center frequency. The FDK values were computed for 7 octave bands based on the results of the WT applied to a signal length of 32s (i,e. 1000 windows). The FDK results for Signals I and III and II and IV are shown in Figures 8(a) and 8(b) respectively. These results clearly highlight the frequency specific differences built into each of the synthetic signals having the same energy and spectra and show that the FDK estimate of a signal is independent of the average spectrum of the signal. The FDK results indicate that the kurtosis estimate across frequencies extracted from the WT can highlight important differences between the nonGaussian and Gaussian components in a signal that are lost in conventional sound level/spectral measurements of a noise environment. Furthermore, the FDK values are higher than 3 (kurtosis for Gaussian conditions) in the octave bands from the region of the spectrum in which the nonGaussian transients were derived.

The four synthesized signals were then run through a conventional electro-acoustic transduction system. The free field acoustic signals were recorded by a 1/2" Bruel & Kjar 4135 microphone and the digitized samples were temporally filtered by a group of FIR filters whose bandwidths were set to successive octave bands. The FDK estimates were computed on the filtered output signals. The results of the FDK computations using the WT are contrasted with the FDK values for the signals obtained using the filter analysis approach in Figure 8. Note that the numerical values of FDK obtained from the WT and the FIR filter approach cannot be directly compared since the WT uses the waveforms from a simulation environment while the results for the FIR filter analysis method were obtained from the calibrated acoustic waveforms measured under field conditions. Nevertheless, it is significant that the FDK from the WT and the FIR filter methods show a similar behavior as a function of frequency.

The FDK values shown in Figure 8 for Signal I are higher than those of Signal II since the transient in Signal I was a shaped impact while the transient in Signal II was a Gaussian noise burst. Kurtosis for an impact is higher than that of a Gaussian noise burst since the impact shows more "impulsiveness" in its amplitude distribution. The same is true when the FDK values of Signal III and Signal IV are compared. Figure 9 further highlights the frequency specificity of the FDK metric obtained from the WT by comparing Signal I and V in which the nonGaussian and Gaussian components were derived from complementary octave bands in the uniform spectral distribution. The FDK statistic can thus indicate not only nonGaussian components in a signal but also their locations in the frequency domain.

Figure 10 shows the FDK values for Signal I using three different probabilities for controlling the occurrence of the impulses. The energy and spectrum are still maintained at the same levels for the different probabilities. With less probability of occurrence of the impulses, fewer impulses will be present in a given length of the temporal waveform, and thus there will be more relative fluctuations in the amplitude distribution because of the longer interpeak interval, resulting in a larger kurtosis estimate.

Comparisons from all the above FDK results, while computed under a limited set of different conditions, indicate that the FDK estimate obtained from the WT provides a frequency specific quantification of the extent of nonstationary fluctuations relative to Gaussian conditions, and that this metric is sensitive to factors such as relative amplitude peaks, transient shapes, and interpeak intervals, etc. Factors such these contribute to the temporal pattern of the signal under consideration and their contributions to the nonGaussian character of the signal are to some extent preserved/quantified in the FDK metric.

(b) Joint peak-interval histogram: Two complex noise waveforms having the same primary impulsive sequence were generated by computer simulation as shown in Figure 11(a). These two waveforms have the identical energy levels and spectra shown in Figure 11(b). Their temporal patterns, as seen in Figure 11(a), are different. Waveform I was generated by a reflectivity sequence whose amplitude reflections and timing delays were randomly distributed. In Waveform II the timing delays of the reflectivity sequence were periodic and the amplitude reflections had a random binary distribution. The reflectivity sequences of these two waveforms are shown in Figure 11(c). These two waveforms were processed by a fourth-order cumulant-based inverse filter to estimate their reflectivity sequence u(k). The inverse filter coefficients were determined by maximizing the magnitude of the fourth-order cumulant of the output sequence, y(k), as shown in Figure 5. The output sequences of these two waveforms are shown in Figure 11(d). These two sequences, resulting from deconvolution by the inverse filter, are the optimum estimates of the reflectivity sequences. Comparison of Figures 11(c) and 11(d) indicates that the estimates provided by the inverse filtering are good estimates of the temporal patterns inherent in the original signals. The joint peak-interval histogram for the two waveforms shown in Figure 11(a) are presented in Figure 12. The amplitude and timing of each spike in the spike train sequences were recorded. The amplitude and temporal variable range was divided into 20 and 16 bins, respectively. The histograms were obtained from a cumulant-based inverse filtering analyses of 1000 windows of the complex noise waveforms. The histograms show different contour shapes for each of the two waveforms. The shape of the histogram for Waveform I, shown in Figure 12(a), is relatively flat and uniform since the amplitude reflections and timing delays are uniformly and normally distributed. The shape of the histogram for Waveform II, shown in Figure 12(b), is periodically spiky and concentrated in the two binary value bins since the timing delays are periodic and the amplitude reflections are randomly binary distributed.

VII. Discussion and Conclusion

This grant has resulted in the development of procedures for extracting new metrics from a sampled noise that differ from conventional metrics which are based on energy and spectral considerations. The new metrics are FDK and the joint peak-interval histogram. The computations for acquiring these metrics were derived from time-frequency analysis, and kurtosis or higher order cumulant based algorithms. The motivation for taking this approach was that statistical computations on the temporal structure are necessary to analyze noise waveforms because of their inherent nonGaussian and nonstationary characteristics. We suggest that, unlike conventional energy-based metrics, FDK and the joint peak-interval histogram can be used as metrics to distinguish among various noise environments whose statistical properties carry different potential for producing hearing loss.

The wavelet transform was used to analyze complex noises having nonstationary and nonGaussian characteristics. WT is a logical choice for processing such signals since the acoustic signals can be analyzed into a time-frequency representation which preserves spectrally specific temporal information. It is particularly suitable for revealing the nonstationary features within signals as compared to traditional spectral analysis techniques. Furthermore, WT can operate on the analyzed signal in a log scaling of frequency rather than a linear scaling which is a major limitation of the short-time Fourier transform (STFT). The human cochlea behaves like a constant-Q system of tuned filters, for which the constant-Q scaling behavior of wavelets appears to be a natural match. Therefore the FDK computations based on WT results can be compared to frequency specific histological and audiometric data scaled logarithmically.

Higher-order cumulant based inverse filtering can be used to decode the temporal structure of a noise that has randomly occurring impulsive components. This technique, derived for solving the blind deconvolution problem, can be used to extract peak amplitudes and timing information on impulse occurrences in a noise waveform without *a priori* knowledge of the impulsive structure (i.e., rise time, duration, repetitive numbers, or frequency contents, etc.). This filtering approach is based on the concept of maximizing the magnitudes of the reponse's normalized cumulant estimates. Compared to the bicepstrum algorithm, being a function of two variables for estimating a bicepstrum, computations of an inverse filtering response's normalized cumulant is performed as functions of one variable. The higher-order cumulant based inverse filtering algorithm is not as computationally complex as the bicepstrum algorithm. With same memory size available to programming, the algorithm for higher-order cumulant based inverse filtering is easier to implement and can process a longer window having more sample points of the temporal sequence (i.e., longer duration). Therefore, higher-order cumulant based inverse filtering can process a complex noise waveform having longer intervals between consecutive impulses.

VIII. Literature cited

Cadzow JA, Li X (1995) Bind deconvolution, Digital signal processing journal, John Wiley, 5(1):3-20.

Cadzow JA (1996) Blind deconvolution via cumulant extrema, IEEE signal processing magazine, 13(3):24-42.

Cooke, M. (1993) Modelling auditory processing and organisation, Cambridge University Press, NY.

Daubechies, I (1989) "Orthonormal bases of compactly supported wavelets," Comm. Pure Applied Math.

Dwyer, R.F.(1984) "Use of the kurtosis statistic in the frequency domain as an aid in detecting random signals," IEEE Journal of Oceanic Engineering, Vol. OE-9(2):85-92.

Erdreich, J. (1986) "Adistribution based definition of impulse noise," J. Acoustic. Soc. Am. 79(4):990-998.

Glasberg, B.R., Moore, B.C. (1990) "Derivation of auditory filter shapes from notched-noise data," hearing Research, 47:103-108.

Hlawatsch, F. and Boudreaux-Bartels, G.F. (1992) "Linear and quadratic time-frequency signal representations," IEEE Signal processing magazine, 21-67.

Holdsworth, J., Mimmo-Smith, I., Patterson, R.D., and Rice, P. (1988) "Implementing a gammatone filter bank," personal communication documents.

Holschneider, M., Kronland-Martinet, R., Morlet, J., and Tchamitchian, Ph. (1989) "A real-time algorithm for signal analysis with the help of the wavelet transform," wavelets: time-frequency methods and phase space, Combes, J.M, Grossman, A., and Tchamitchian, ph. Eds. Berlin:Springer, IPITI,286-297.

Hsueh KD, Hamernik RP (1990) A generalized approach to random noise synthesis: theory and computer simulation. J. Acoust. Soc. Am. 87:3:1207-1217.

Hsueh KD, Hamernik RP (1991) Performance characteristics of a phase domain approach to random noise synthesis. Noise Control Eng. J. 18-32.

International standards organization, ISO 3891, DAD1 (1978) "Procedure for describing aircraft noise heard on the ground: measurement of noise from helicopters for certification," Geneva.

Lei SF, Ahroon WA and Hamernik RP (1994) The application of frequency and time domain kurtosis to the assessment of hazardous noise exposures. J. Acous. Soc. Am. 96:3:1435-1444.

Mallat, S.G.(1989) "A theory of multiresolution signal decomposition: the wavelet representation," IEEE Trans. Pattern Anal. Machine Intell., 2:674-693.

Morlet, J. et al., (1982) "Wave propagation and sampling theory-Part II: sampling theory and complex waves," Geophysics, 47:2: .

Patterson,R.D., Robinson, K., Holdsworth, J., Mckeown, D., Zhang, C., and Allerhand, M. (1992) "Complex sounds and auditory images," Auditory physiology and perception, advances in biosciences, Cazals, Y, Demany, L and Horner, K. eds., Pergamon press, 429-446.

Shalvi O, Weinstein E(1990) New criteria for blind deconvolution of nonminimum phase systems, IEEE Trans. Information Theory, 36(2):312-321.

Shanno DF (1970) Conditioning of quasi-newton methods for function minimization Mathematics of Computing, 24:647-656.

Shensa, M.J. (1992) "The discrete wavelet transform: wedding the A-trous and Mallat algorithms," IEEE Trans. Signal Processing, 40(10):2464-2482.

Yang, X., Wang, K., and Shamma, S.A. (1992) "Auditory representations of acoustic signals," IEEE Trans. Information Theory, 38:2:824-839.

IX. Publications

Lei, S-F., Hamernik, R.P. (1998). Application of the wavelet transform and higher-order cumulant-based inverse filtering to the quantification of non-Gaussian noise for use in estimating hearing hazards. Paper presented at the 1998 Midwinter Meeting of the Association for Research in Otolaryngology, St. Petersburg Beach, Florida, February, 1998.

Abstract: The foundation of the ISO-1999 standard for estimating NIHL in noise-exposed groups is tied to two postulates that form the basis of: (a) an age correction procedure and (b) the use of an energy metric (L_{eq}) to quantify the exposure. This leads to a straight-forward relation; NIHL = f(age, L_{eq}). Implicit in such a formulation is that temporal variables associated with a noise exposure are not significant for the production of NIHL. This is contrary to the accumulating experimental data that suggest that energy may be a necessary but not sufficient metric for the evaluation of noise exposures. For example, Lei et al. [JASA 96:1435 (1994)] have shown that the statistical properties of a nonGaussian noise, reflected in the kurtosis statistic, which incorporates both temporal and peak properties of a signal in the time domain [$\beta(t)$] and spectral effects when computed on the frequency domain signal [$\beta(f)$], are highly correlated with the magnitude and distribution of sensory cell loss. In this paper we describe an approach to and present a rationale for the analysis of noise environments that incorporates the wavelet transform and higher-order cumulant based inverse filtering to obtain $\beta(t)$, $\beta(f)$, and the joint peak-interval histogram.

Lei, S.-F. and Hamernik, R.P. (1998). Construction of a joint peak-interval histogram using higher-order cumulant based inverse filtering. Paper submitted to the 1998 International Converence on Acoustics, Speech and Signal Processing, Seattle, WA, May 12-15.

Abstract: Conventional metrics used to quantify signals in noise/hearing research rely primarily on time-averaged energy and spectral analyses. Such metrics, while appropriate for Gaussian-distributed waveforms, are of limited value in the more complex sound environments encountered in industrial/military settings that have nonGaussian and nonstationary-distributed waveforms. Recent research has shown that metrics incorporating the temporal characteristics of a waveform are needed to evaluate hazardous acoustic environments for purposes of hearing conservation. The joint peak-interval histogram is a prospective candidate for use in such an application. This paper shows that the joint peak-interval histogram can be obtained from an estimation of the temporal pattern of a complex noise waveform by using higher-order cumulant-based inverse filtering.

Lei, S-F. and Hamernik, R.P. (1998). Application of higher-order cumulant-based inverse filtering to the quantification of impulsive noise for hearing conservation. Paper to be presented at the Eighth IEEE Digital Signal Processing Workshop, Bryce Canyon National Park, Utah, August 9-12, 1998.

Abstract: Conventional metrics used to quantify acoustic waveforms in noise-induced hearing loss (NIHL) research rely primarily on time-averaged energy and spectral analyses. Such metrics, while appropriate for Gaussian-distributed waveforms, are of limited value in the more complex sound environments encountered in industrial/military settings that have impulsive characteristics. The joint peak-interval histogram is a prospective candidate for use in such an application. This paper shows that the joint peak-interval histogram can be obtained from an estimation of the temporal pattern of a complex noise waveform by using higher-order cumulant-based inverse filtering.

Lei, S.-F. and Hamernik, R.P. (1996). Extraction of frequency domain kurtosis from nonGaussian and nonstationary signals using the wavelet transform. International Symposium on Optical Science, Engineering and Instrumentation: Wavelet Applications in signal and image processing. Proc. SPIE 2825:785-795.

Abstract: Conventional metrics to quantify signals used in hearing research are primarily derived from time-averaged energy and spectral analyses. Such metrics, while appropriate for Gaussian signals, are of limited value in more complex sound environments. Many of the sounds encountered in industrial/military environments have nonGaussian and nonstationary distributed waveforms. These signals may have the same energy and spectra as those of a continuous Gaussian signal, yet they can produce very different effects on the auditory system. This result has led to efforts to develop additional metrics, incorporating the temporal characteristics of a signal, that could be useful in evaluating hazardous acoustic environments. This paper suggests that frequency domain kurtosis (FDK) obtained from an application of the wavelet transform may be useful in such an application.

Lei, S-F., Ahroon, W.A. and Hamernik, R.P. (1996): The application of frequency and time domain kurtosis to the assessment of complex, time varying noise exposures. In: *Scientific Basis of Noise-Induced Hearing Loss*, ed. A. Axelsson, H. Borchgrevink, R. P. Hamernik, P.A. Hellstrom, D. Henderson, R.J. Salvi. Thieme Medical Publishers, Inc.

Abstract: Industrial noise is typically characterized by high-level noise transients that are superimposed on a continuous noise background producing a complex (non-Gausian) temporal signal. High kurtosis exposures have been shown to pose a higher risk of hearing loss to the repeatedly exposed individual than an equivalent energy Gaussian noise. Current measurement practice relies on a time averaged energy metric, the L_{eq}, to characterize noise exposures. The L_{eq} will be inadequate for any exposures in which temporal variables are important in determining the extent of trauma. This paper shows that, for continuous noise exposures having the same L_{eq} and spectra, the statistical properties of the signal are important in the prediction of acoustic trauma. The results indicate that the kurtosis computed on both the time domain signal, $\beta(t)$, and the frequency domain signal, $\beta(f)$ in conjunction with the L_{eq} can order the magnitude of acoustic trauma and reflect its frequency specificity. These conclusions are based upon the results obtained from 114 chinchillas exposed to one of twelve different noises in a five-day, asymptotic threshold shift producing exposure paradigm. Hearing thresholds were obtained using brainstem evoked auditory responses and sensory cell populations were quantified using surface preparation histology.

Lei, S-F., Hamernik, R.P. (1995). Wavelet Transform and Frequency Domain Kurtosis: Application to Assessment of Hearing Hazard from Noise Exposure. Proceedings *IEEE Applications of Signal Processing to Audio and Acoustics*. pp.1.4.1-3, New Paltz, NY, IEEE publishers, NJ.

Abstract: Research on the effects of noise on the auditory system has shown that the frequency domain kurtosis (FDK) statistic could be a useful metric in quantifying a noise environment for hearing conservation purposes. Joint time-frequency analytical methods used in signal processing may be of use in the extraction of such information from an exposure environment characterized by nonstationary signals. This paper shows that the

FDK metric can be efficiently computed by applying the wavelet transform to the analysis of an acoustic signal.

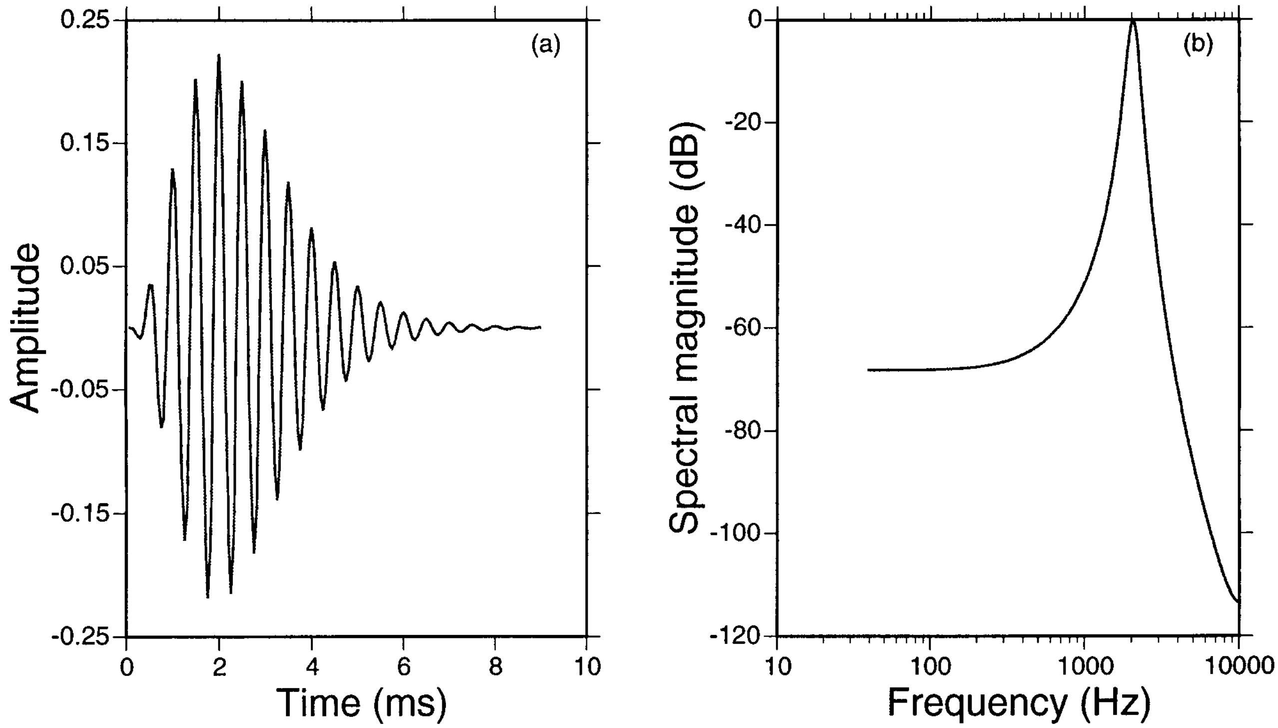

Figure 1. (a) Impulse response of a fourth-order gammatone filter. (b) Frequency response of a fourth-order gammatone filter. f_c = 2000 Hz.

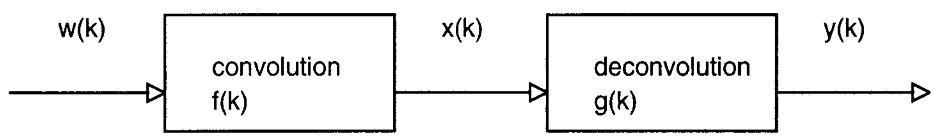

Figure 2. Block diagram of deconvolution operator to recover the input w(k) from observed sequence x(K) alone.

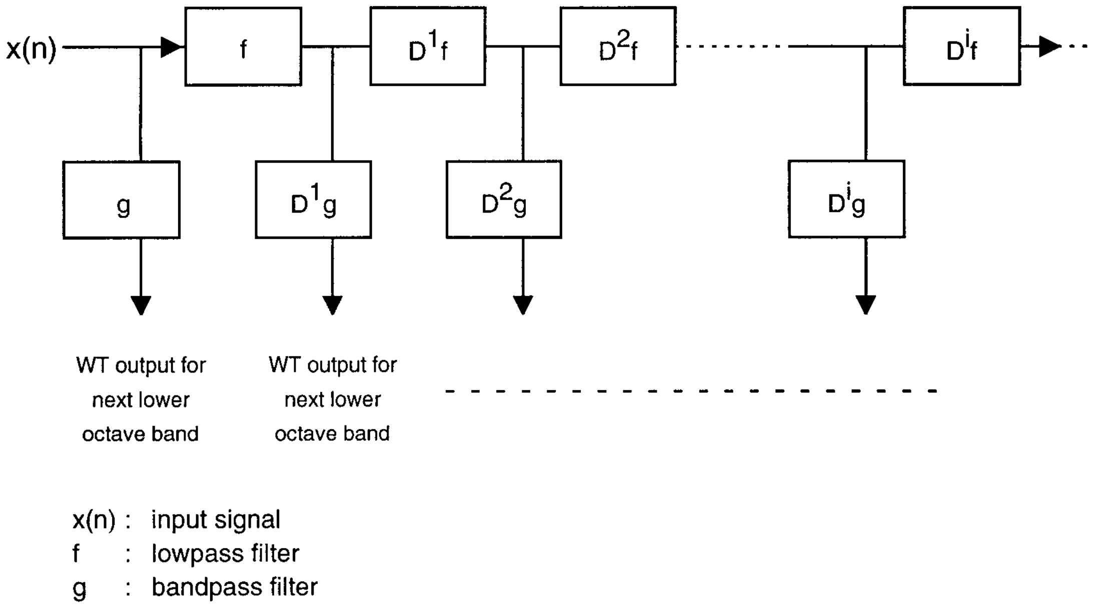

Figure 3. A-trous algorithm discrete wavelet transform. The filters D^if are obtained from f by inserting 2^i-1 zeros between each pair of filter coefficients.

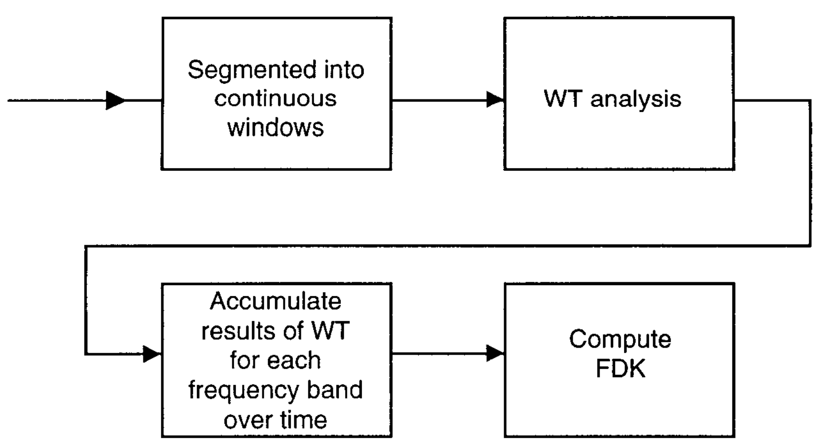

Figure 4. Block diagram of FDK analysis based on WT on octave bands.

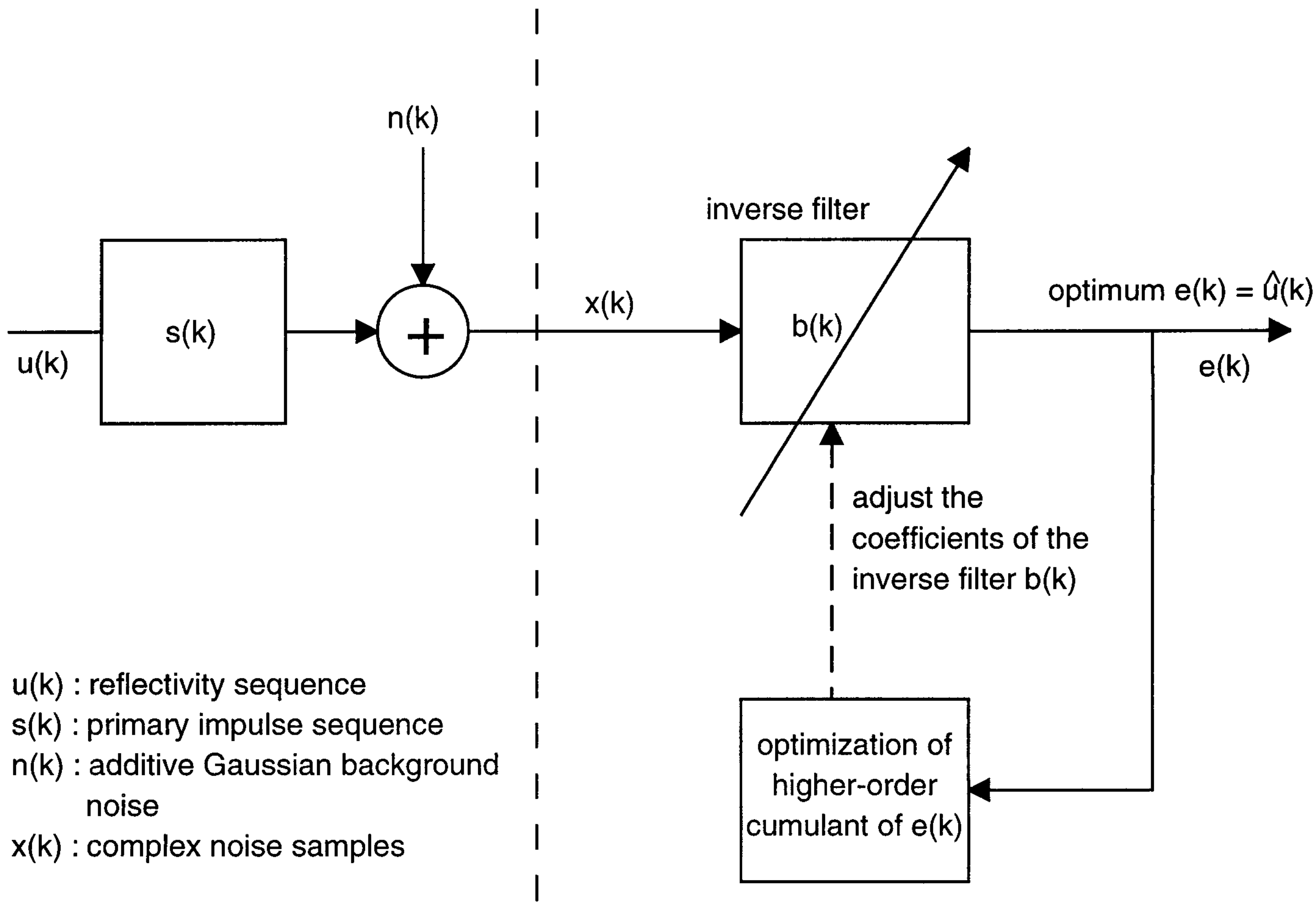

Figure 5. A higher-order cumulant based inverse filter used to estimate the reflectivity sequence in a complex noise.

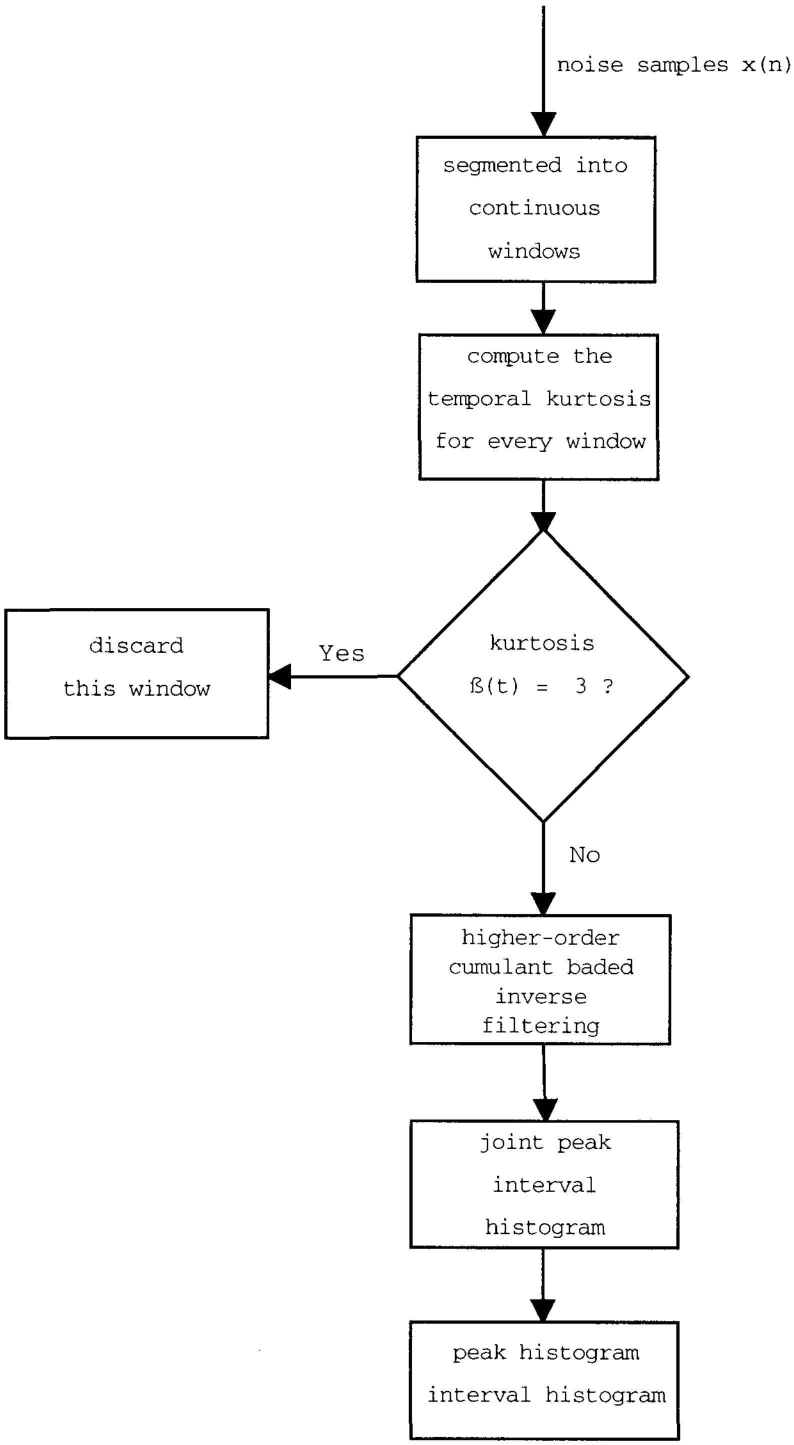

Figure 6. Procedural steps for joint peak interval histogram

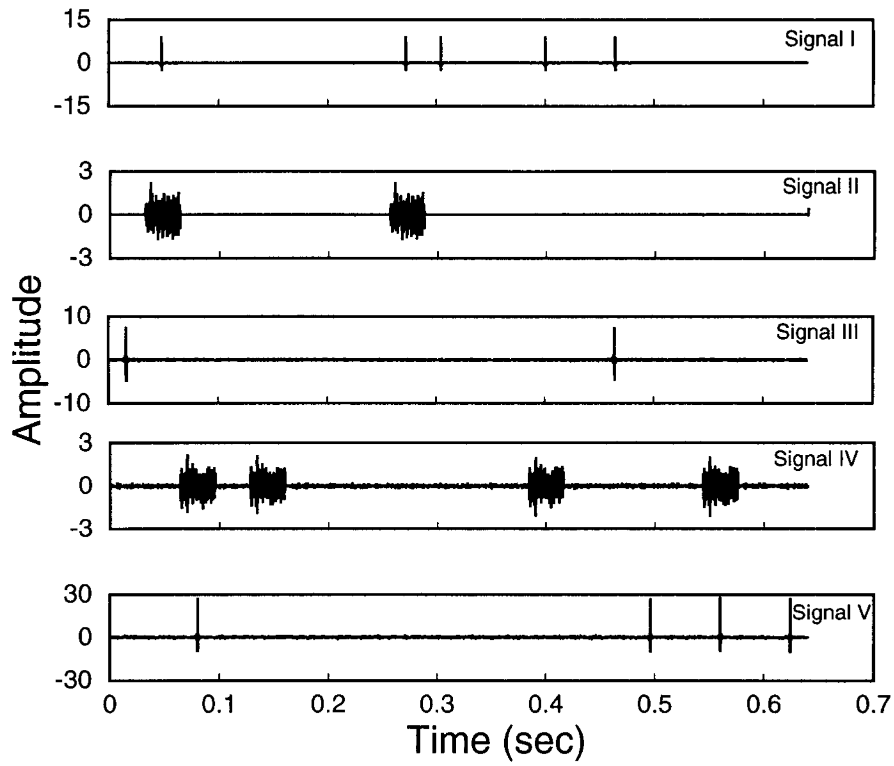

Figure 7(a) Temporal waveforms of Signals I through V

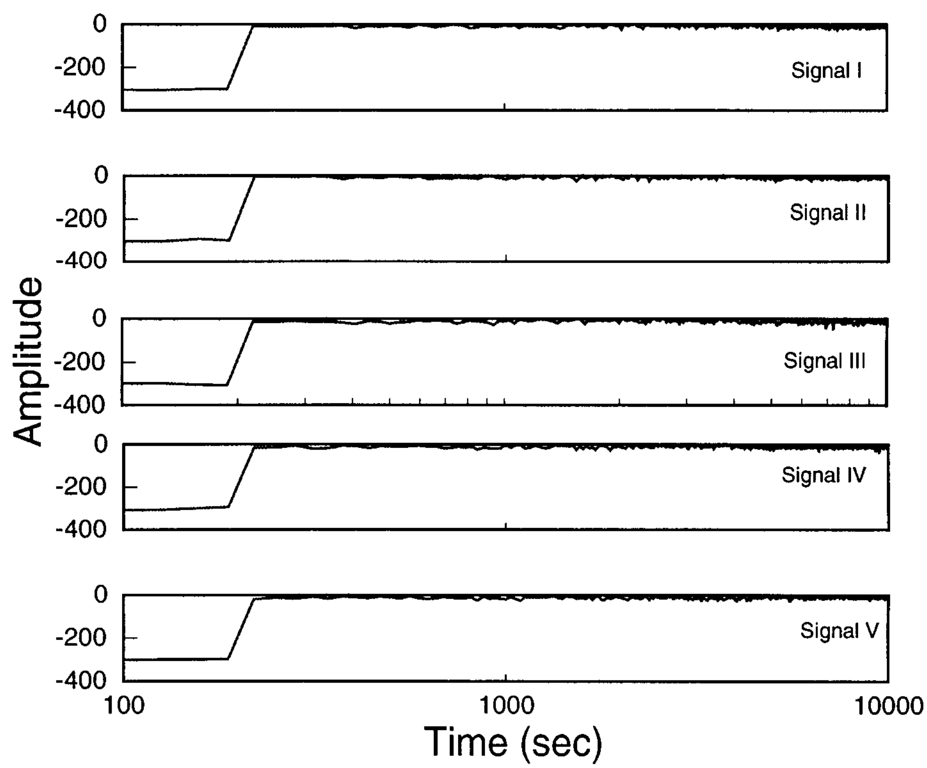

Figure 7(a) Temporal waveforms of Signals I through V

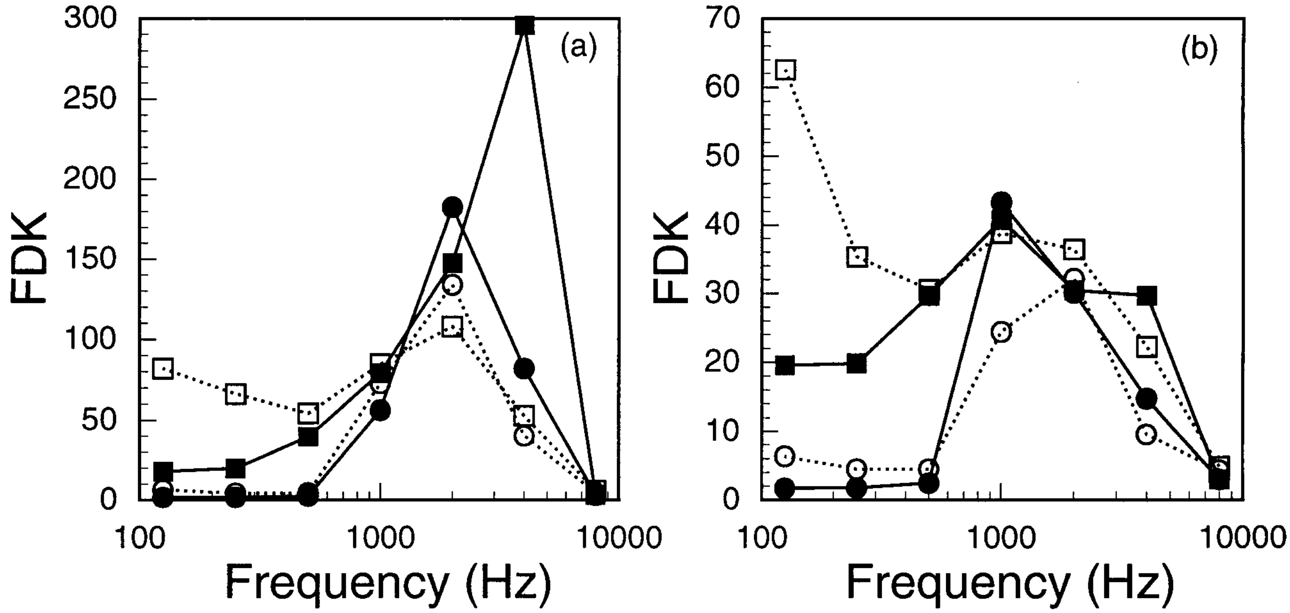

Figure 8. (a) FDK values of Signals I (■,□) and III (●,O); (b) FDK values of Signals II (■,□) and IV (●,O). Solid symbols - wavelet transforms and open symbols - filter analysis approach.

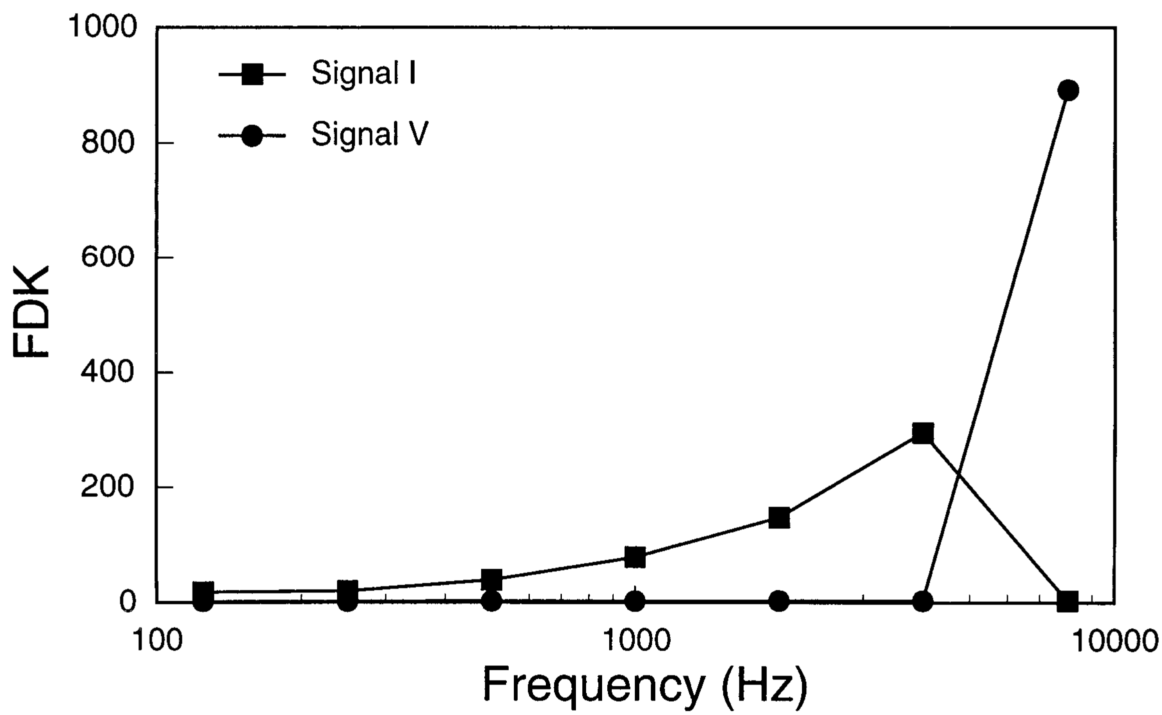

Figure 9. FDK values of Signal I and Signal V.

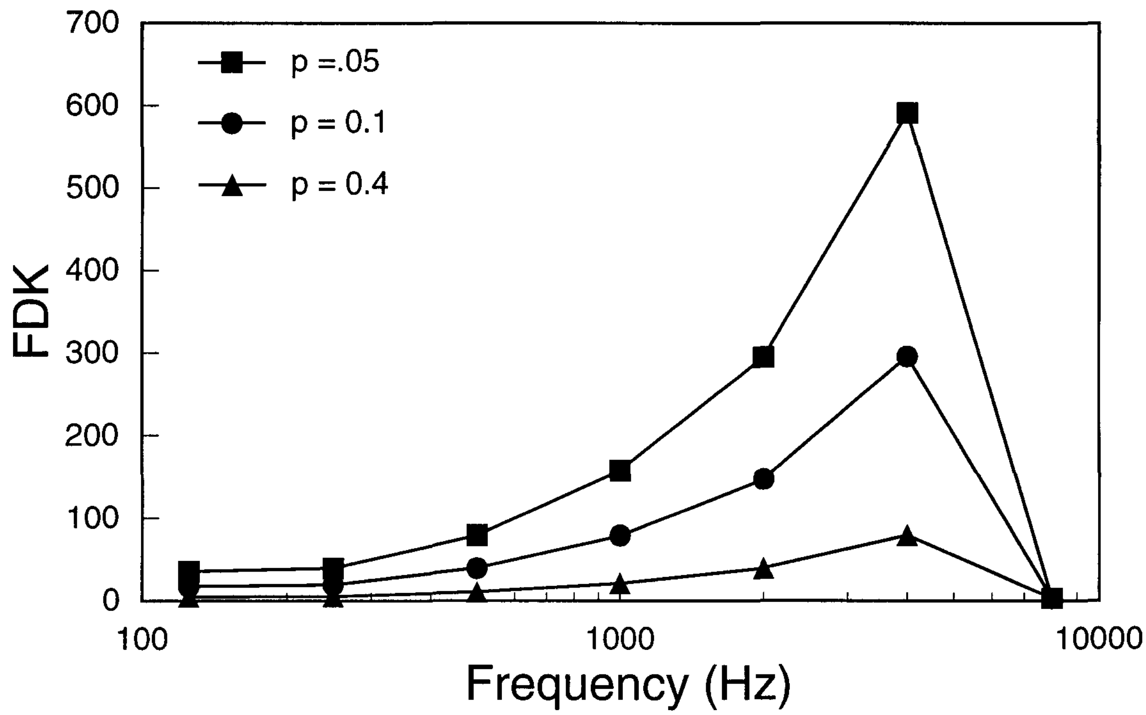

Figure 10. FDK values of signal I with different probabilities of impacts occurring.

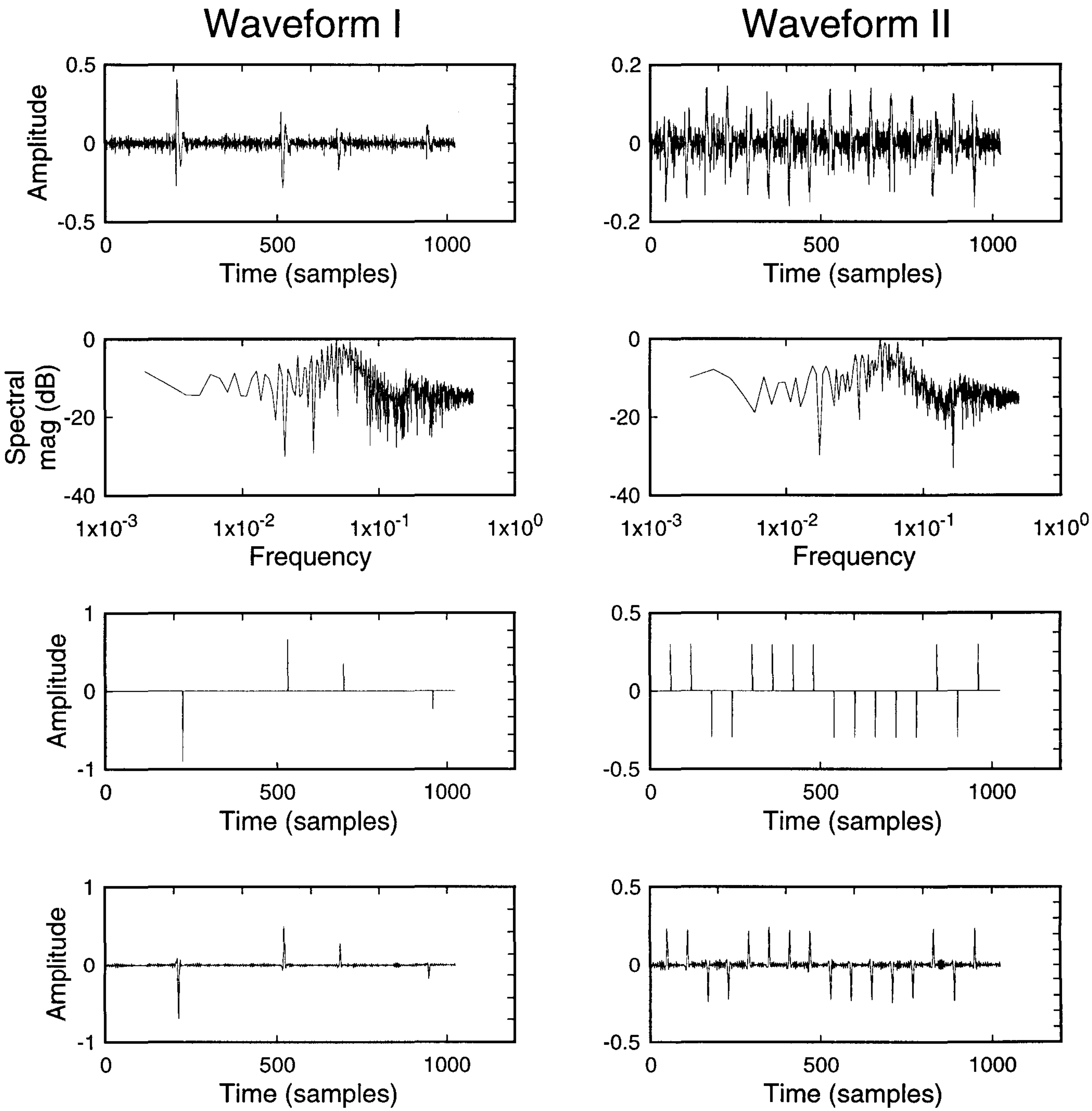

Figure 11. (a) Examples of two complex noise waveforms having different temporal structures. (b) Spectra of each of the temporal waveforms. (c) The reflectivity sequences of each of the temporal waveforms. (d) The reflectivity sequences for each of the waveforms estimated from a fourth-order cumulant based inverse filter analysis.

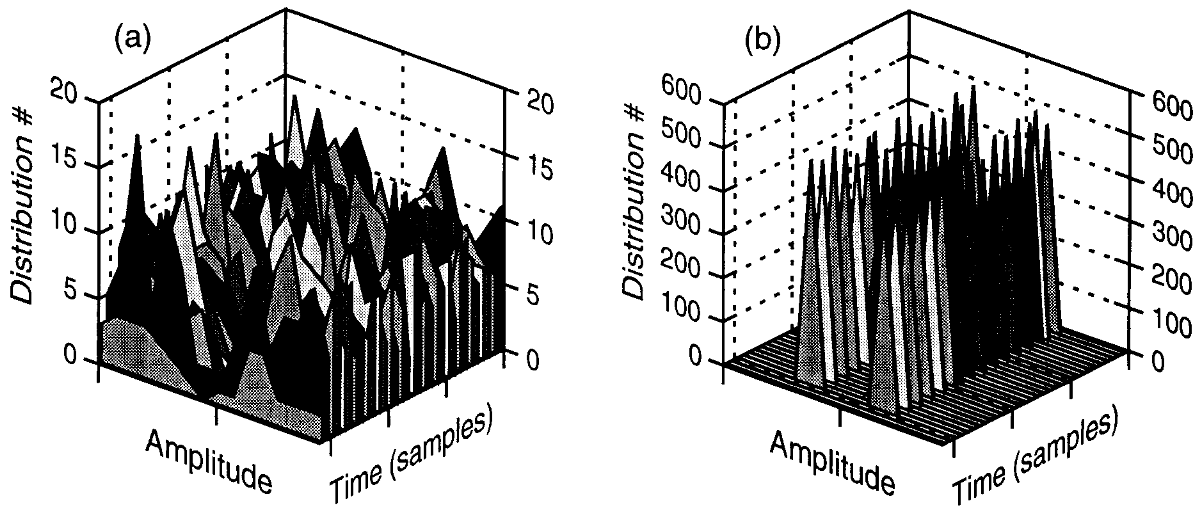

Figure 12. Joint peak-interval histograms of Waveforms I (a) and II (b).